Desalination and Water Treatment
www.deswater.com

doi: 10.5004/dwt.2017.21490

92 (2017) 152–159
October

TiO_2 nanoparticles containing phthalocyanine as a visible light driven photocatalyst for degradation of thionine acetate in synthetic wastewater

Azadeh Ebrahimian Pirbazari

Fouman Faculty of Engineering, College of Engineering, University of Tehran, P.O. Box 43515-1155, Fouman 43516-66456, Iran, Tel. +981334734927; Fax: +981334737228; email: aebrahimian@ut.ac.ir

Received 25 May 2017; Accepted 23 September 2017

ABSTRACT

In this research, preparation and photocatalytic performance of cobalt phthalocyanine tetrasulfonate sensitized TiO_2 nanoparticles (CoPcTs/TiO_2) for the degradation of thionine (TH) under visible light was reported. The prepared samples were characterized by X-ray diffraction, Fourier-transform infrared spectra, diffuse reflectance spectroscopy, nitrogen physisorption and transmission electron microscopy techniques. The obtained data revealed that the sensitized TiO_2 nanoparticles have pure anatase phase with crystal size of approximately 9.5 nm and surface area of 141 $m^2 g^{-1}$. The experimental parameters such as catalyst dose, initial TH concentration and initial pH were studied. Maximum photodegradation of TH (more than 90%) was achieved within 120 min with the catalyst loading of 0.5 g L^{-1} and initial TH concentration of 10 mg L^{-1}, in the condition of neutral pH under visible light. Only 40% degradation of the TH was obtained in the presence of pure TiO_2. The photocatalytic degradation reactions followed first-order kinetics and the experiential rate constants changed with TH concentrations.

Keywords: Nanoparticles; TiO_2; Cobalt phthalocyanine; Thionine; Kinetic; Mechanism

1. Introduction

TiO_2, as an inorganic semiconductor, is widely used for photocatalytic purification and photoelectric conversion of organic and inorganic pollutants from water and air. TiO_2 has several advantages such as its photostablility, reusability, nontoxicity and inexpensiveness. In addition, it has a reasonable photocatalytic activity under UV light irradiation for environmental applications [1]. Despite their features, the low quantum yield of TiO_2 in the aqueous solution, fast recombination rate of photoexcited hole/electron pairs and its high band gap energy, limit its practical applications. Many efforts have been made to enhance the utilization of visible light or solar energy and inhibit the recombination of photogenerated electron–hole pairs such as metal or nonmetal doping, semiconductors coupling, dye sensitization, noble metal deposition and surface modification [2–5]. Among them, dye sensitization is considered one of the most efficient methods to develop practical applications [6]. Some reports confirm that the visible photocatalytic activity of TiO_2 can be effectively improved by choosing an appropriate sensitizer, such as coumarin [7], porphyrin [8] or phthalocyanines [9]. Phthalocyanines and porphyrins complexes have attracted more attention due to their low cost so that, these sensitizers and their derivatives are particularly attractive owing to their strong absorption in the region of 400–450 nm (Soret band) and in the region of 500–700 nm (Q-bands). Furthermore, they have high thermal, chemical stability and high efficiency for visible light conversion into chemical energy [10]. The conduction band (CB) of TiO_2 is very close to the LUMO orbital energy of the phthalocyanine complex. After visible light absorption by phthalocyanine, the molecules are excited and transformed to higher energy state and injected electrons to CB of TiO_2. The surface adsorbed oxygen scavenged the electrons and yielded some active species such as $O_2^{\bullet -}$, $HO^{\bullet}$ [11]. The literature survey showed that there were several reports on the preparation of TiO_2 catalysts containing phthalocyanine by impregnation [12–16], causing heterogeneous molecular distribution of the phthalocyanine molecules in the TiO_2 network. Some authors reported the incorporation of phthalocyanine complexes into TiO_2 gel [17–19]. In previous studies, the performance

of TiO_2 nanoparticles has been sensitized by cobalt phthalocyanine tetrasulfonate (CoPcTs) for heterogeneous photocatalytic degradation of 2,4-dichlorophenol, 4-chlorophenol and methylene blue has been investigated [9,20,21]. The heterogeneous photocatalytic degradation of thionine (TH) by this sample has not been reported so far. The TH dye, as an organic pollutant, is commonly used as a sensitizer in photographic processes, laser components, photographic filter layers and chemotherapy [22]. Hence, searching for an efficient photocatalyst for degrading this harmful and widely used dye remains a considerable challenge. In this work, CoPcTs sensitized TiO_2 nanoparticles were prepared by sol-gel method. The synthesized sample was characterized by several analyses including: X-ray diffraction (XRD), transmission electron microscopy (TEM), nitrogen physisorption and diffuse reflectance spectroscopy (DRS). The photocatalytic activity of the samples was investigated in degrading TH dye under visible light.

2. Experimental

2.1. Materials and reagents

CoPcTs was synthesized, purified and characterized according to the method proposed by Weber and Bush [23]. Tetraisopropyl orthotitanat (No. 8.21895, Merck, Germany), ethanol, acetylacetone and deionized water were used for TiO_2 synthesis. High-purity TH (No. 149346, Merck) was used as a probe molecule for photocatalytic tests.

2.2. Preparation of CoPcTs/TiO_2 nanoparticles

CoPcTs/TiO_2 and pure TiO_2 were prepared by the method described in [9]. Solution A: 20 mL $Ti(OC_3H_7)_4$, 20 mL ethanol and 1.62 mL acetylacetone were stirred for 30 min at room temperature. Solution B: 50 mg CoPcTs, 80 mL ethanol and 2 mL H_2O were stirred for 30 min. Solution B was added into solution A and colored solution C was obtained. Solution C was transferred into an autoclave, and then heated to 240°C at a heating rate of approximately 2°C min^{-1} and the temperature was maintained for 6 h. After this time, the obtained solid was washed with ethanol and water and dried at 150°C for 2 h in air. This photocatalyst is labelled as CoPcTs/TiO_2. Solution C without CoPcTs was also prepared to obtain pure TiO_2.

2.3. Characterization

XRD patterns were recorded using Philips PW 1840 diffractometer with Cu-Kα radiation (40 kV, 40 mA), scan rate of 0.02° 2θ/s within the range of 2θ of 20°–80°. Diffuse reflectance spectra were recorded by a UV-2100 Shimadzu Spectrophotometer, equipped with an integrating sphere assembly. TEM studies were conducted with a Hitachi-H-8100 instrument (accelerating voltage up to 200 kV, LaB6 filament). The samples were prepared by being dispersed in an ultrasonic bath for 20 min in ethanol. The nitrogen physisorption measurements were performed with a Quantachrome Autosorb-1-MP. Fourier-transform infrared (FT-IR) spectra were recorded with a Shimadzu FT-IR spectrometer (Model 8400).

2.4. Photocatalytic degradation monitoring

UV-visible light photocatalytic activities of the prepared samples were evaluated by degrading model organic pollutant of TH acetate dye. The photocatalytic reactions were studied under a 500 W Halogen lamp (Osram, Germany). A visible (Halogen, ECO OSRAM, 500 W) lamp was used as an irradiation source (its emitting wavelength ranges from 350 to 800 nm with the predominant peak at 575 nm). The UV-visible light focused on a 100 mL aqueous solution of TH (10 mg L^{-1}) and photocatalyst. The suspension was magnetically stirred first in the darkness for 10 min before photocatalysis reaction, ensuring that the adsorption/desorption of TH reaches a stable equilibrium. Every interval time of 20 min, small aliquots (2 mL) were withdrawn and filtered to remove the photocatalyst particles and analyzed by Rayleigh UV-2601 UV/Vis spectrophotometer (λ_{max}= 598 nm). Calibration curves were constructed for TH degradation, and all experiments were performed three times to verify the repeatability of the results.

3. Result and discussion

3.1. Characterization of synthesized samples

3.1.1. Powder X-ray analysis

Fig. 1 shows the XRD patterns of the prepared samples. The diffraction at 2θ = 24.88°, 37.42°, 47.66°, 53.49°, 54.51°, 62.29°, 68.55°, 69.97° and 74.69° confirms that the TiO_2 particles are polycrystalline with an anatase structure. TiO_2-based photocatalysts used in rutile and anatase structures, and anatase structure showed much higher photocatalytic activity than the rutile one [24]. The XRD pattern of CoPcTs/TiO_2 sample (Fig. 1(b)) did not exhibit any diffraction for CoPcTs complex and it may be confirmed by complete dispersion of CoPcTs molecules into TiO_2 nanoparticles during the hydrolysis of tetraisopropyl orthotitanat or low loading quantity. The crystal size of TiO_2 was calculated according to Scherrer equation from the width of the anatase (1 0 1) diffraction.

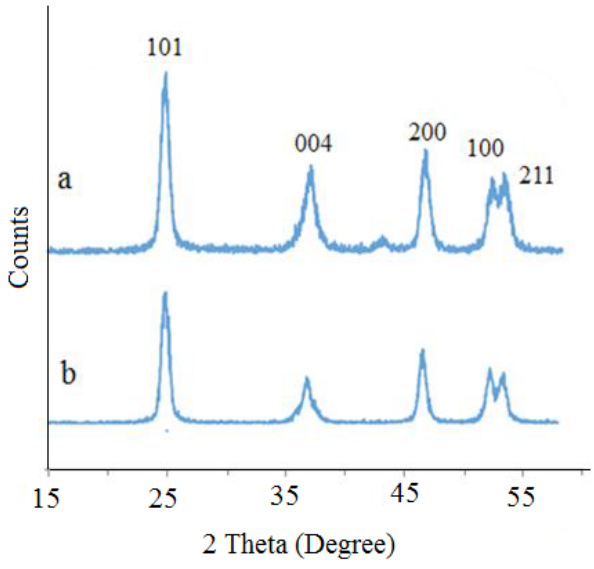

Fig. 1. Powder XRD patterns of (a) TiO_2, (b) CoPcTs/TiO_2.

$$D = K\lambda/\beta \cos\theta \quad (1)$$

In this equation, D(h k l) is the crystal thickness, λ is the wavelength of the X-ray, β is the peak width at half-maximum and θ is the Bragg angle. The crystal size for the pure TiO_2 and CoPcTs/TiO_2 samples are found to be 9 and 9.5 nm, respectively.

3.1.2. Diffuse reflectance spectroscopy

Fig. 2 shows the diffuse reflectance spectra (A) and Kubelka-Munk function (B) of the prepared samples. The diffuse reflectance spectrum of TiO_2 (Fig. 2(A)) showed that there was no more absorption in the visible region. Fig. 2(B) shows the diffuse reflectance spectrum of CoPcTs/TiO_2 sample, and there was great absorption in the visible wavelength range (600–700 nm). The two absorption peaks in the visible region were attributed to the Q absorption bands originating from $\pi \rightarrow \pi^*$ transitions of CoPcTs complex and extended the CoPcTs/TiO_2 spectrum to the visible region. The monomeric and aggregated CoPcTs species showed absorption peaks at 680 and 620 nm, respectively [25]. The band gap energy from the DR spectra calculated according to Eq. (2) for the synthesized samples:

$$[F(R)\ h\upsilon]^{0.5} = A\ (h\upsilon - E_g) \quad (2)$$

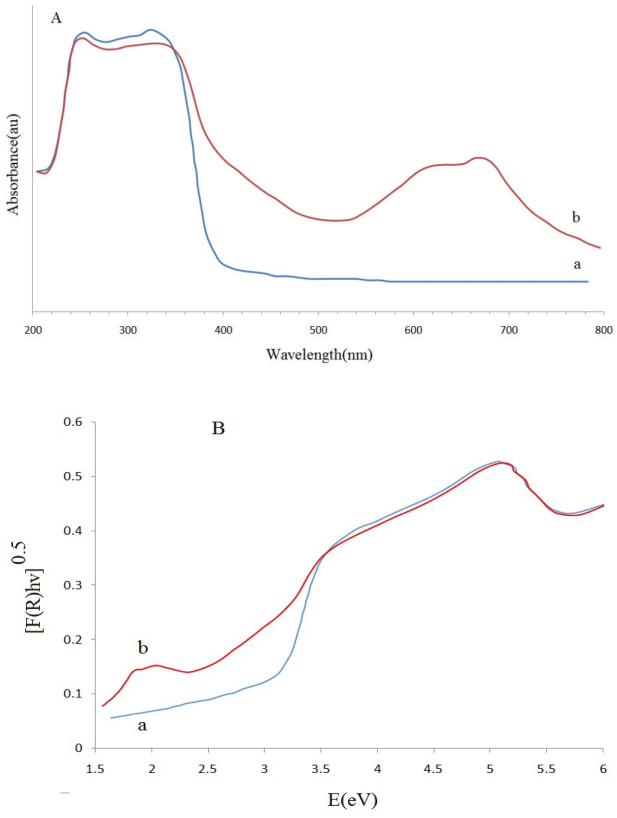

Fig. 2. (A) Diffuse reflectance spectra and (B) Kubelka-Munk plots for the band gap energy calculation of (a) TiO_2 and (b) CoPcTs/TiO_2.

where A is constant, F(R) is the function of Kubelka-Munk and E_g is the band gap. The band gap energy was obtained to be 3.01 and 2.5 eV for pure TiO_2 and CoPcTs/TiO_2 samples, respectively.

3.1.3. TEM analysis

TEM analysis was used for the size and morphology analysis of the prepared samples. The TEM micrographs (Fig. 3) show excellent dispersibility for irregular spheral TiO_2 nanoparticles with the size in the range from 9 to 10 nm. The dispersibility of the nanoparticles enhanced the photocatalytic efficiency of the photocatalyst.

3.1.4. FT-IR analysis

Fig. 4 shows the FT-IR spectra of the CoPcTs, pure TiO_2 and CoPcTs/TiO_2. The vibrations in the range of 1,700–1,000 cm^{-1} (Fig. 4(c)) are attributed to the characteristic vibrations of CoPcTs complex [26]. The FT-IR spectrum of CoPcTs/TiO_2 (Fig. 4(b)) which shows the vibration at ~1,400 cm^{-1} confirms the presence of CoPcTs and due to low amount of CoPcTs, the intensity of this vibration is weak [27]. The sulfonic groups of CoPcTs showed vibration at approximately 670 cm^{-1} (Fig. 4(c)) [28] and disappeared in the FT-IR spectrum of CoPcTs/TiO_2 sample due to the covalent bonding formation between sulfonic groups of CoPcTs and hydroxyl group of TiO_2. Vargas et al. [29] reported this covalent bonding and FT-IR analysis showed the characteristic vibrations at 1,150 and 1,210 cm^{-1} for stretching vibration of S–O–Ti bond. Ti–OH bond showed vibrations at ~3,400, 2,930 and 2,850 cm^{-1} [30]. The bending vibration of OH at ~1,630 cm^{-1} for chemisorbed and/or physisorbed water molecules detected for the samples. There is the stretching vibrations of Ti–O–Ti bond in the range of 700–500 cm^{-1} [31].

3.1.5. Nitrogen physisorption

Fig. 5 shows the N_2 adsorption/desorption isotherms of the prepared samples. The prepared samples exhibit the type IV sorption isotherm according to the IUPAC classification [32]. Table 1 summarized the obtained data from nitrogen physisorption. We calculated the specific surface areas and pore volumes from the Brunauer–Emmett–Teller (BET) method, pore volumes and radii were obtained from Barrett–Joyner–Halenda model. Decrease in the specific surface area of the CoPcTs/TiO_2 sample may be explained by CoPcTs

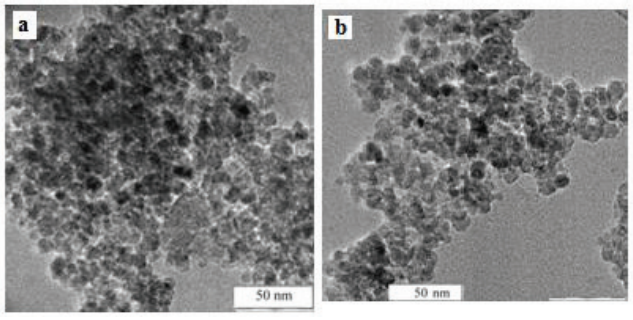

Fig. 3. TEM micrograph of (a) TiO_2 and CoPcTs/TiO_2.

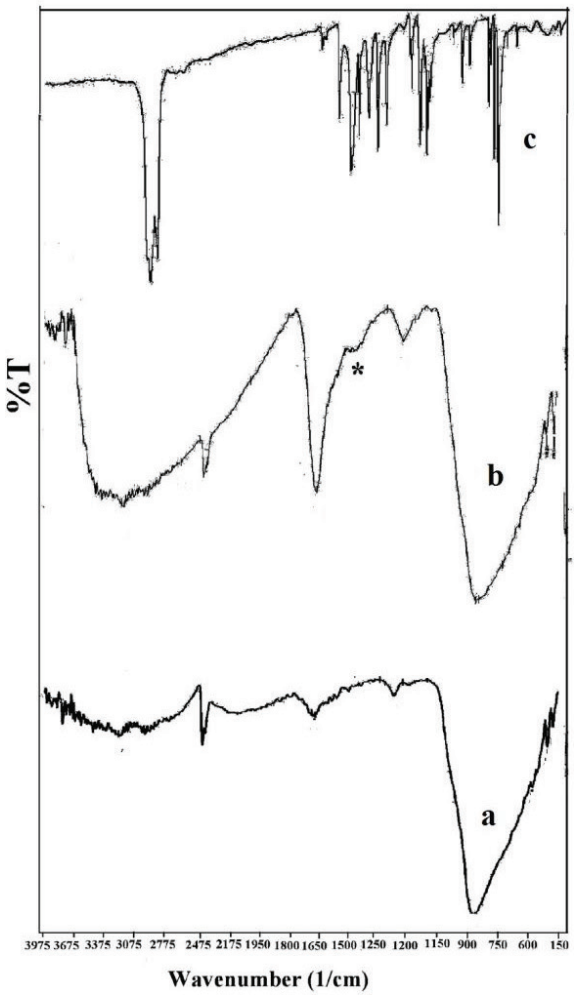

Fig. 4. FT-IR spectra of (a) TiO_2, (b) CoPcTs/TiO_2 and (c) CoPcTs.

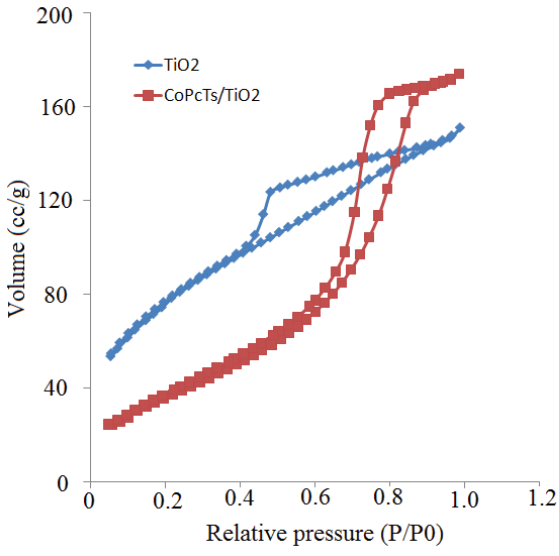

Fig. 5. N_2 adsorption–desorption isotherms for TiO_2, and CoPcTs/TiO_2.

molecules incorporated into TiO_2 nanoparticles and reduce the surface area of TiO_2. The average pore diameter for CoPcTs/TiO_2 sample was obtained to be 76 Å and the size of the phthalocyanine ligand is (20 × 20 Å). Moreover, the pore volume of CoPcTs/TiO_2 sample is greater than that of pure TiO_2. These observations can confirm that tetrasulfophthalocyanine acts as a bridging ligand and controls the hydrolysis process of the TIP, resulting in CoPcTs/TiO_2 sample with mesoporous structure and high surface area.

3.2. Study of different parameters on photocatalytic degradation of TH

3.2.1. Catalyst dose

An important factor which can significantly influence the photocatalytic degradation rate is catalyst dose [33]. To determine the optimum catalyst dose, some experiments were conducted in the presence of different amounts of CoPcTs/TiO_2 sample from 0.1 to 1.5 g L^{-1} of the TH solution (TH concentration = 10 mg L^{-1}, pH = 7) (Fig. 6). Fig. 6 demonstrates that the rate of photocatalytic degradation of TH increases linearly with catalyst loading up to 0.5 g L^{-1} reaching a maximum of degradation at a catalyst dose of 1.0 g L^{-1} and, then, decreases as the catalyst dose increases. The photocatalytic degradation of other organic pollutants also showed similar dependency on catalyst loading [34]. According to the work by Wu et al. [35], the higher photocatalytic degradation needs more dosage of the catalyst. This can be attributed to the increase in the total active surface area, increase of light absorption and hence availability of more active sites on the catalyst surface. However, at higher dosage, beyond the optimal limit, the dispersed particles of the catalyst block the visible light passage and increase the light scattering [36]. Therefore, further increase in the loading of catalyst will have no effect on the photocatalytic degradation rate. The obtained results showed that, the optimum catalyst dose was chosen as 0.5 g L^{-1} for subsequent experiments.

3.2.2. Effect of pH

One of the highly important operation parameters for photocatalytic degradation reaction is pH. Hoffmann et al. [37] reported that the pH lower than the pH of the zero point charge (pH_{zpc}) of TiO_2 would favor the interaction of TiO_2 with anionic electron donors and electron acceptors and the pH higher than the pH of the pH_{zpc} of TiO_2 would favor the interaction of TiO_2 with cationic electron donors and electron acceptors. Therefore, an appropriate value of solution pH was needed for photocatalytic degradation reactions. In this work, pH_{zpc} was determined for TiO_2 and CoPcTs/TiO_2 according to the procedure described in [38]. The pH_{zpc} was obtained to be 5.5 and 5.9 for TiO_2 and CoPcTs/TiO_2, respectively. Fig. 7 shows the effect of pH value on the photocatalytic degradation of TH in the presence of CoPcTs/TiO_2. The obtained results showed that the difference of pH value had a strong influence on the photocatalytic degradation of TH changing the surface properties of the catalyst. TH is a cationic dye and its adsorption is favored in alkaline solution (higher pH values). At higher pH value, the surface of the CoPcTs/TiO_2 has negative charge and more TH molecules can be adsorbed

Table 1
Textural and structural parameters of the prepared samples

Sample	S_{BET} ($m^2 g^{-1}$)	Pore $volume_{BET}$ ($cm^3 g^{-1}$)	Pore $volume_{BJH}$ ($cm^3 g^{-1}$)	Pore diameter (Å)
TiO_2	280	0.23	0.24	38
$CoPcTs/TiO_2$	141	0.27	0.29	76

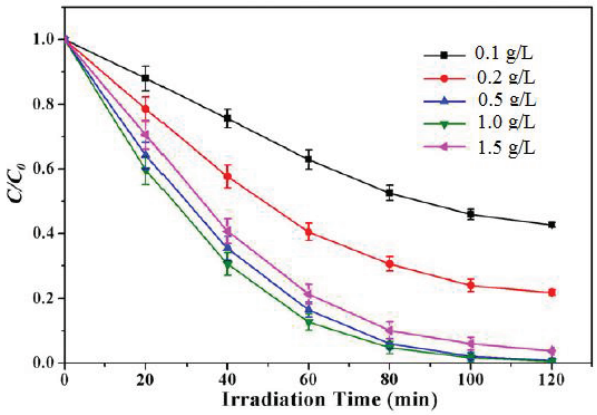

Fig. 6. Effect of the $CoPcTs/TiO_2$ dose on photocatalytic degradation of TH ([TH]: 10 mg L^{-1}; pH = 7).

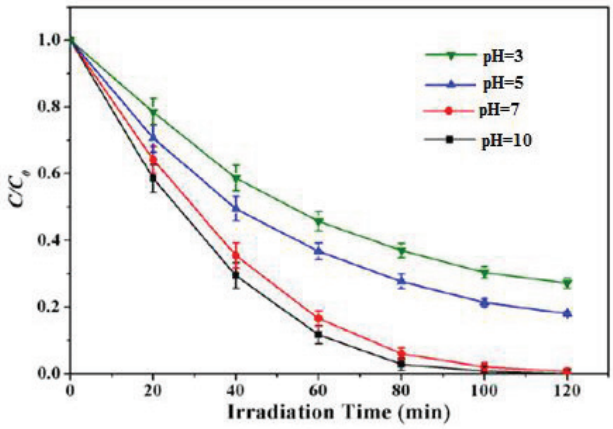

Fig. 7. Effect of initial pH on photocatalytic degradation of TH (catalyst dose: 0.5 g L^{-1}; [TH]: 10 mg L^{-1}).

on the surface through the electrostatic interactions and decolorization of TH molecules occurring under visible light irradiation [39]. The optimum pH value was chosen to be 7 for subsequent experiments (Fig. 7).

3.2.3. Effect of initial concentration of dye

Fig. 8 shows the effect of TH initial concentration on photocatalytic degradation efficiency. At higher initial concentration of TH, the photocatalytic degradation efficiency decreases. The key species in the photocatalytic degradation process are hydroxyl radicals (•OH) and the adsorption of TH molecules on the photocatalyst surface sites increases with the TH concentration increase, decreasing the competitive adsorption of OH^- on the same sites [31]. It will

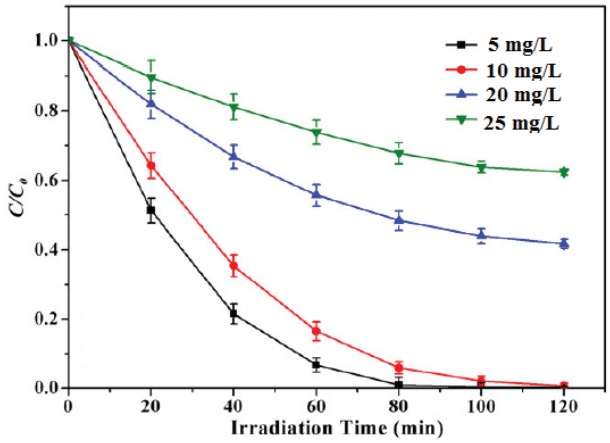

Fig. 8. Effect of initial concentration on photocatalytic degradation of TH (catalyst dose: 0.5 g L^{-1}; pH = 7).

finally lead to a lower formation rate of •OH radical [40]. By increasing the adsorbed molecules on the catalyst surface, the dye molecules absorbed the light much more than the catalyst did, having an inhibitive effect and decreasing the rate of photocatalytic degradation of the TH [41]. The initial TH concentration was selected as 10 mg L^{-1} for further experiments.

3.2.4. Recyclability of $CoPcTs/TiO_2$

The recyclability of the $CoPcTs/TiO_2$ sample was studied during a four-cycle experiment for the TH degradation. Recycling experiments (Fig. 9) showed reduction in activity from 97% to 63% after four cycles. The reduction of the photocatalytic performance could be explained by probable attack of OH radicals to the phthalocyanine molecules in $CoPcTs/TiO_2$ sample or by permanent adsorption of intermediate species formed during photocatalytic degradation of the TH that would compete with the TH for the reactive species generated (hydroxyl radical or peroxy free radical) from the irradiated photocatalyst [9].

3.2.5. Kinetic study

Table 2 shows the kinetic parameters for the TH photocatalytic degradation. The obtained results showed that the photocatalytic degradation of the TH is first-order reaction and its kinetics is expressed as $\ln(C_0/C) = k_{obs}t$. In this equation k_{obs} (min^{-1}) is the apparent rate constant, C_0 and C are the initial concentration and concentration of the TH at reaction time t. The initial reaction rate of photocatalytic degradation of the TH is faster at higher initial concentrations and the rate constants decrease by increasing the TH initial concentrations.

These results may be explained due to limited lifetime of active species formed during the photocatalytic degradation reaction. The active oxygen species such as: $OH^{\bullet}$ and $O_2^{\bullet-}$ are formed on the surface of the immobilized photosensitizer (CoPcTs) and would not go far away [42] and would react preferably with the TH dye molecules near the photocatalyst surface. Thus, the initial degradation rate is faster at high initial concentrations of the TH.

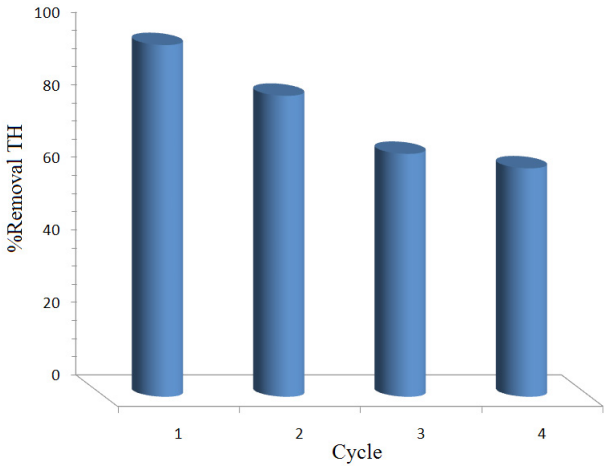

Fig. 9. Recyclability of the catalyst for photocatalytic degradation of TH after four successive cycles (catalyst dose: 0.5 g L^{-1}; [TH]: 10 mg L^{-1}; pH = 7; irradiation time: 120 min).

3.2.6. Proposed mechanism for TH degradation

TiO_2 is well known for its electronic structure, acting as a good photocatalyst under UV irradiation. It has a filled valance band (VB) and an empty CB [43]. After absorption photons with energy 3.2 eV or higher, electrons in the VB are excited to CB, leaving holes in the VB, and forming electron–hole pairs. The excited-state electron–holes pairs can react with a stable electron acceptor and donor to produce radicals such as $O_2^{\bullet-}$ and $HO^{\bullet}$. These radicals are extremely active and can oxidize or reduce pollutants to the mineral end-products [1,37]. In the present work, both components, TiO_2 and CoPcTs complex can absorb the photons at their interface, since the CB of TiO_2 and the lowest unoccupied molecular orbital (LUMO) level of CoPcTs complex are matched well for the charge transfer. Therefore, the electrons can be injected into the CB of TiO_2 nanoparticles [18] react with oxygen to form some reactive oxygen species being capable of attacking organic pollutants and degrading them [44,45]. Therefore, the TH could be degraded through more than one pathway [46]. Fig. 10 shows the proposed mechanism for photocatalytic degradation of the TH in the presence of CoPcTs/TiO_2.

Table 2
First-order reaction rate constants and correlation coefficients for different concentrations of TH

TH initial concentration (mg L^{-1})	k_{obs} (min^{-1})	Initial reaction rate (mg L^{-1} min^{-1})	$t_{1/2}$ (min)	R^2
5	0.0241	0.1205	28.75	0.9986
10	0.0168	0.1680	41.25	0.9916
15	0.0139	0.2085	49.85	0.9974
20	0.0129	0.2580	53.72	0.9991
25	0.0115	0.2875	60.26	0.9974

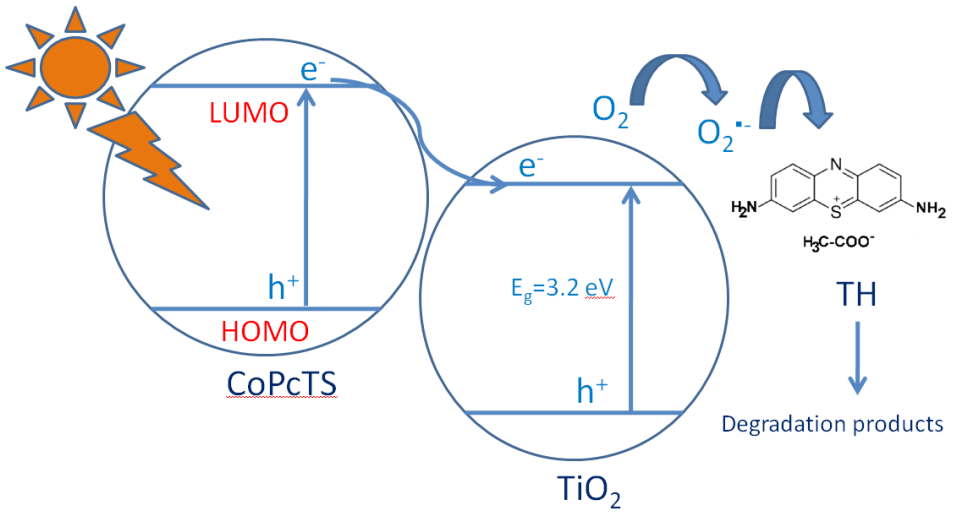

Fig. 10. Proposed mechanism for photocatalytic degradation of TH in the presence of CoPcTs/TiO_2 photocatalyst.

4. Conclusion

TiO_2 nanoparticles containing CoPcTs complex were prepared by hydrothermal method and characterized by different techniques including XRD, FT-IR, TEM, DRS and nitrogen physisorption. The FT-IR and nitrogen physisorption results confirmed that CoPcTs molecules were attached on the surface of TiO_2 nanoparticles through covalent SO_2–O–TiO_2 bonds. The photocatalytic performance of the prepared photocatalyst was tested for the photocatalytic degradation of the TH under visible light. Different parameters such as pH, catalyst dose and initial concentrations of the TH were investigated on the photocatalytic degradation rate. The photocatalytic degradation rate of TH follows first-order reaction kinetics and the reaction is completed within 120 min (concentration of TH: 10 mg L^{-1} and catalyst dose: 0.5 g L^{-1}) under visible light.

Acknowledgments

The author wishes to acknowledge the financial support of Iran National Science Foundation (Grant No: 92025598). Also, the author is so thankful to University of Tehran for supporting this research.

References

[1] A. Fujishima, T.N. Rao, D.A. Tryk, Titanium dioxide photocatalysis, J. Photochem. Photobiol., C, 1 (2000) 1–21.
[2] S.H. Kang, W. Lee, H.S. Kim, Effects of CdS sensitization on single crystalline TiO_2 nanorods in photoelectrochemical cells, Mater. Lett., 85 (2012) 74–76.
[3] J. Yu, Y. Hai, M. Jaroniec, Photocatalytic hydrogen production over CuO-modified titania, J. Colloid Interface Sci., 357 (2011) 223–228.
[4] V. Mendonc, O.F. Lopes, R.P. Fregonesi, T.R. Giraldic, C. Ribeirod, TiO_2-SnO_2 heterostructures applied to dye photodegradation: the relationship between variables of synthesis and photocatalytic performance, Appl. Surf. Sci., 298 (2014) 182–191.
[5] J. Zhang, L.J. Xu, Z.Q. Zhu, Q.L. Liu, Synthesis and properties of (Yb, N)-TiO_2 photocatalyst for degradation of methylene blue (MB) under visible light irradiation, Mater. Res. Bull., 70 (2015) 358–364.
[6] C. Huang, Y. Lv, Q. Zhou, S. Kang, X. Li, J. Mu, Visible photocatalytic activity and photoelectrochemical behavior of TiO_2 nanoparticles modified with metal porphyrins containing hydroxyl group, Ceram. Int., 40 (2014) 7093–7098.
[7] S. Palmas, A.D. Pozzo, M. Mascia, A. Vacca, P.C. Ricci, Sensitization of TiO_2 nanostructures with Coumarin 343, Chem. Eng. J., 211–212 (2012) 285–292.
[8] Sh. Murphy, C. Saurel, A. Morrissey, J. Tobin, M. Oelgemöller, K. Nolan, Photocatalytic activity of a porphyrin/TiO_2 composite in the degradation of pharmaceuticals, Appl. Catal., B, 119–120 (2012) 156–165.
[9] A. Ebrahimian, M.A. Zanjanchi, H. Noei, M. Arvand, Y. Wang, TiO_2 nanoparticles containing sulphonated cobalt phthalocyanine: preparation, characterization and photocatalytic performance, J. Environ. Chem. Eng., 21 (2014) 484–494.
[10] C.C. Leznoff, A.B.P. Lever, Eds., Phthalocyanines. Properties and Applications, VCH Publ. Inc., New York, 1996, p. 4.
[11] G. Mele, L. Palmisano, G. Dyrda, R. Słota, Photocatalytic degradation of 4-nitrophenol in aqueous suspension by using polycrystalline TiO_2 impregnated with lanthanide double-decker phthalocyanine complexes, J. Phys. Chem. B, 111 (2007) 6581–6588.
[12] G. Mele, R. Del Sole, G. Vasapollo, G. Marcı´, L. Palmisano, J.M. Coronado, M.D. Herna´ndez-Alonso, C. Malitesta, M.R. Guascito, TRMC, XPS, and EPR characterizations of polycrystalline TiO_2 porphyrin impregnated powders and their catalytic activity for 4-nitrophenol photodegradation in aqueous suspension, J. Phys. Chem. B, 109 (2005) 12347–12352.
[13] G. Mele, R. Del Sole, G. Vasapollo, E. García-López, L. Palmisano, M. Schiavello, Photocatalytic degradation of 4-nitrophenol in aqueous suspension by using polycrystalline TiO_2 impregnated with functionalized Cu(II)–porphyrin or Cu(II)–phthalocyanine, J. Catal., 217 (2003) 334–342.
[14] G.O. Granados, C.A.M. Paèz, F.O. Martıńez, E.A. PaézMozo, Photocatalytic degradation of phenol on TiO_2 and TiO_2/Pt sensitized with metallophthalocyanines, Catal. Today, 107–108 (2005) 589–594.
[15] L. Li, B. Xin, Photogenerated carrier transfer mechanism and photocatalysis properties of TiO_2 sensitized by Zn(II) phthalocyanine, J. Cent. South Univ. Technol., 17 (2010) 218–222.
[16] W. Fa, L. Zan, Ch. Gong, J. Zhong, K. Deng, Solid-phase photocatalytic degradation of polystyrene with TiO_2 modified by iron (II) phthalocyanine, Appl. Catal., B, 79 (2008) 216–223.
[17] K.T. Ranjit, I. Willner, S. Bossmann, A. Braun, Iron(III) phthalocyanine-modified titanium dioxide: a novel photocatalyst for the enhanced photodegradation of organic pollutants, J. Phys. Chem. B, 102 (1998) 9397–9403.
[18] Z. Wang, W. Mao, H. Chen, F. Zhang, X. Fan, G. Qian, Copper(II) phthalocyanine tetrasulfonate sensitized nanocrystalline titania photocatalyst: synthesis in situ and photocatalysis under visible light, Catal. Commun., 7 (2006) 518–522.
[19] Z. Wang, H. Chen, P. Tang, W. Mao, F. Zhang, G. Qian, X. Fan, Hydrothermal in situ preparation of the copper phthalocyanine tetrasulfonate modified titanium dioxide photocatalyst, Colloid. Surf., A, 289 (2006) 207–211.
[20] A. Ebrahimian Pirbazari, Sensitization of TiO_2 nanoparticles with cobalt phthalocyanine: an active photocatalyst for degradation of 4-chlorophenol under visible light, Procedia Mater. Sci., 11 (2015) 622–627.
[21] M. Muhler, A. Ebrahimian, M.A. Zanjanchi, Sensitization of TiO_2 Nanoparticles with Sulphonated Cobalt Phthalocyanine: An Active Photocatalyst for Methylene Blue Degradation under Visible Light, Proc. 4th International Conference on Nanostructures (ICNS4), Kish Island, Iran, 2012.
[22] F.P. Schafer, Dye Lasers, Springer-Verlag, Berlin, 1973.
[23] J.H. Weber, D.H. Bush, Complexes derived from strong field ligands. XIX. Magnetic properties of transition metal derivatives of 4,4′,4″,4‴- tetrasulfophthalocyanine, Inorg. Chem., 4 (1965) 469–471.
[24] K. Tanaka, M.F.V. Capule, T. Hisanaga, Effect of crystallinity of TiO_2 on its photocatalytic action, Chem. Phys. Lett., 29 (1991) 73–76.
[25] V. Iliev, V. Alexiev, L. Bilyarska, Effect of metal phthalocyanine complex aggregation on the catalytic and photocatalytic oxidation of sulfur containing compounds, J. Mol. Catal. A: Chem., 137 (1999) 15–22.
[26] R. Seoudi, G.S. El-Bahy, Z.A. El Sayed, FTIR, TGA and DC electrical conductivity studies of phthalocyanine and its complexes, J. Mol. Struct., 753 (2005) 119–126.
[27] P. Karandikar, A.J. Chandwadkar, M. Agashe, N.S. Ramgir, S. Sivasanker, Liquid phase oxidation of alkanes using Cu/Co-perchlorophthalocyanine immobilized MCM-41 under mild reaction conditions, Appl. Catal., A, 297 (2006) 220–230.
[28] M.R. Nabid, S. Asadi, M. Shamsianpour, R. Sedghi, S. Osati, N. Safari, Oxidative polymerization of 3,4-ethylenedioxythiophene using transition-metal tetrasulfonated phthalocyanine, React. Func. Polym., 70 (2010) 75–80.
[29] E. Vargas, R. Vargas, O. Núñez, A TiO_2 surface modified with copper(II) phthalocyanine-tetrasulfonic acid tetrasodium salt as a catalyst during photoinduced dichlorvos mineralization by visible solar light, Appl. Catal., B, 156–157 (2014) 8–14.
[30] Y. Wang, Y. Huang, W. Ho, Biomolecule-controlled hydrothermal synthesis of C–N–S-tridoped TiO_2 nanocrystalline photocatalysts for NO removal under simulated solar light irradiation, J. Hazard. Mater., 169 (2009) 77–87.
[31] E. Bae, W. Choi, Highly enhanced photoreductive degradation of perchlorinated compounds on dye-sensitized metal/TiO_2 under visible light, Environ. Sci. Technol., 37 (2003) 147–152.

[32] K.S.W. Sing, D.H. Everett, R.A.W. Haul, L. Moscou, R.A. Pierotti, Reporting physisorption data for gas/solid systems with special reference to the determination of surface area and porosity, Pure Appl. Chem., 57 (1985) 603–619.
[33] M. Beyrhouty, A.B. Sorokin, S. Daniele, L.G. Hubert-Pfalzgraf, Combination of two catalytic sites in a novel nanocrystalline TiO_2–iron tetrasulfophthalocyanine material provides better catalytic properties, New J. Chem., 29 (2005) 1245–1248.
[34] N. Daneshvar, D. Salari, A.R. Khataee, Photocatalytic degradation of azo dye acid red 14 in water: investigation of the effect of operational parameters, J. Photochem. Photobiol., A, 157 (2003) 111–116.
[35] X. Wang, P. Wu, Zh. Huang, N. Zhu, J. Wu, P. Li, Zh. Dang, Solar photocatalytic degradation of methylene blue by mixed metal oxide catalysts derived from ZnAlTi layered double hydroxides, Appl. Clay Sci., 95 (2014) 95–103.
[36] E. Evgenidou, K. Fytianos, I. Poulios, Semiconductor-sensitized photodegradation of dichlorvos in water using TiO_2 and ZnO as catalysts, Appl. Catal., B, 59 (2005) 81–89.
[37] M.R. Hoffmann, S.T. Martin, W. Choi, D.H. Bahneman, Environmental applications of semiconductor photocatalysis, Chem. Rev., 95 (1995) 69–96.
[38] P. Panneerselvam, N. Morad, K.A. Tan, Magnetic nanoparticle (Fe_3O_4) impregnated onto tea waste for the removal of nickel(II) from aqueous solution, J. Hazard. Mater., 186 (2011) 160–168.
[39] Q. Xiao, J. Zhang, Ch. Xiao, Zh. Si, X. Tan, Solar photocatalytic degradation of methylene blue in carbon-doped TiO_2 nanoparticles suspension, Solar Energy, 82 (2008) 706–713.
[40] A. Akyol, H.C. Yatmaz, M. Bayramoglu, Photocatalytic decolorization of remazol red RR in aqueous ZnO suspensions, Appl. Catal., B, 54 (2004) 19–24.
[41] K.M. Parida, N. Baliarsingh, B.S. Patra, J. Das, Copperphthalocyanine immobilized Zn/Al LDH as photocatalyst under solar radiation for decolorization of methylene blue, J. Mol. Catal. A: Chem., 267 (2007) 202–208.
[42] L. Wu, A. Li, G. Gao, Zh. Fei, Sh. Xu, Q. Zhang, Efficient photodegradation of 2,4-dichlorophenol in aqueous solution catalyzed by polydivinylbenzene-supported zinc phthalocyanine, J. Mol. Catal. A: Chem., 269 (2007) 183–189.
[43] F. Wang, Sh. Min, Y. Han, L. Feng, Visible-light-induced photocatalytic degradation of methylene blue with polyaniline-sensitized TiO_2 composite photocatalysts, Superlattices Microstruct., 48 (2010) 170–180.
[44] L. Song, R.L. Qiu, Y.Q. Mo, D.D. Zhang, H. Wei, Y. Xiong, Photodegradation of phenol in a polymer-modified TiO_2 semiconductor particulate system under the irradiation of visible light, Catal. Commun., 8 (2007) 429–433.
[45] H.C. Liang, X.Z. Li, Visible-induced photocatalytic reactivity of polymer–sensitized titania nanotube films, Appl. Catal., B, 86 (2009) 8–17.
[46] A. Houas, H. Lachheb, M. Ksibi, E. Elaloui, Ch. Guillard, J.-M. Herrmann, Photocatalytic degradation pathway of methylene blue in water, Appl. Catal., B, 31 (2001) 145–157.